

Characterization of Pyrene-Labeled Arborescent Polystyrenes Using Fluorescence Quenching Techniques

Randy S. Frank,¹ Gerhard Merkle,² and Mario Gauthier*

Institute for Polymer Research, Department of Chemistry, University of Waterloo, Waterloo, Ontario, Canada N2L 3G1

Received April 7, 1997; Revised Manuscript Received June 23, 1997

ABSTRACT: The chain segmental density and diffusional properties of arborescent (highly branched) polystyrenes were investigated by labeling the polymers with pyrene and observing their quenching behavior. A series of arborescent polymers with short ($5000 \text{ g}\cdot\text{mol}^{-1}$) branches and a linear polymer were investigated. Nitrobenzene and nitrated linear polystyrene were used as quenchers for the pyrene fluorescence. For the nitrobenzene quenching experiments, quencher diffusion coefficients were calculated using the Smoluchowski equation. Comparison of the diffusion coefficients indicates a reduced diffusion rate for small molecules inside arborescent polystyrenes relative to the linear polymer and a decreasing trend with increasing generation number. Quenching experiments with linear nitrated polystyrene led to downward curvature in the Stern–Volmer plots, suggesting that a portion of the chromophores were not accessible to the quencher groups. The fractional Stern–Volmer model was applied, and the quenching rate constants and fraction of accessible chromophores were obtained. The arborescent samples had reduced quenching rate constants, and the fraction of accessible chromophores decreased for higher generation polymers.

Introduction

Dendritic polymers are a new class of branched molecules which are the object of intense research efforts.³ These compounds are typically obtained from controlled condensation reactions of AB_n -type monomers. Many different methods have been suggested for the synthesis of dendritic polymers, including divergent, convergent, and one-pot schemes. An alternate approach, also leading to a dendritic structure, uses polymer chains rather than small molecules as building blocks.^{4,5} In the arborescent polymer synthesis,⁴ chloromethyl grafting sites are introduced on a linear polystyrene chain and reacted with living polystyryl anions to give a comb (generation $G = 0$) structure. Cycles of functionalization and grafting can be repeated to produce higher generation ($G = 1, 2, \dots$) polymers, as shown in Figure 1. This approach has a number of advantages over the condensation-type dendrimer syntheses. Since chains obtained by anionic polymerization are used as building blocks, high molecular weight polymers of uniform size are obtained in few reaction steps. It is also possible to control the structure of the graft polymers by varying the density of grafting sites on the backbone polymer and the size of the branches. The influence of structure on the physical properties of arborescent polymers has been demonstrated using light scattering,⁶ viscometry, differential scanning calorimetry,⁷ and atomic force microscopy.⁸ In all cases, increased structural rigidity was observed for higher generation polymers and when the size of the side chains was decreased.

Fluorescence techniques are very useful for the characterization of polymers. They have been applied in the study of a wide range of processes such as end-to-end cyclization, micellization, diffusion within latex particles, phase separation in polymer blends, and polymerization kinetics.⁹ These investigations were accomplished either by addition of a small molecule fluorescent probe to a polymer system, or by attachment of fluo-

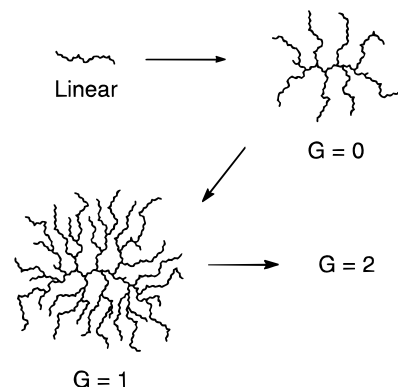


Figure 1. Generation scheme in the synthesis of arborescent graft polymers.

rescent labels to the polymer chains and observation of their fluorescence characteristics. Fluorescence measurements also provided useful information on the morphology of condensation-type dendritic polymers.¹⁰

The aim of this work is to further characterize arborescent polymers using fluorescence quenching experiments. Emphasis is on probing the structure of arborescent polymers, in terms of segmental density and molecular interpenetrability. Nitrobenzene was used to investigate the diffusion of small molecules inside the graft polymers. Nitrated linear polystyrene served to probe the amount of interpenetration between arborescent and other polymer molecules. The results of the experiments can be rationalized in terms of the influence of structural differences among the labeled polymers on their quenching behavior.

Experimental Methods

Materials. The polymers investigated were prepared by an anionic grafting technique described earlier.⁴ A branching functionality of ca. 15 side chains per backbone chain and branches of $5000 \text{ g}\cdot\text{mol}^{-1}$ were used for each generation. Polymers of generations 0 through 3 were investigated. Chloromethyl methyl ether (CMME) was prepared from hexanoyl chloride and dimethoxymethane.¹¹ Carbon tetrachloride (Anachemia, reagent) for the chloromethylation reaction was dried by refluxing and distillation over phosphorus pentoxide.

* Abstract published in *Advance ACS Abstracts*, August 15, 1997.

Recrystallization from a 20:1 ethanol–water mixture was used to purify 1-pyrenecarboxaldehyde (Aldrich, 99%). The corresponding alcohol, 1-pyrenemethanol, was prepared by reduction of the aldehyde with sodium borohydride (Aldrich, 99%) in tetrahydrofuran (THF; Caledon, reagent), followed by four recrystallizations from ethyl acetate. Sodium hydride (Aldrich, 60% dispersion in mineral oil) was used as received. *N,N*-Dimethylformamide (DMF; BDH, ACS reagent) was vacuum-distilled from calcium hydride (Aldrich, 90–95%) immediately before use. Tetrahydrofuran used in the fluorescence measurements was distilled and stored in the dark under nitrogen to avoid peroxide formation.

Polystyrene Samples Characterization. The molecular weight and polydispersity data for the polymers studied were determined using size exclusion chromatography (SEC) and static light scattering. Samples of the branches were obtained by removing an aliquot of the living polystyryl anions prior to the grafting reaction. The weight-average molecular weight, M_w , and polydispersity index ($PDI = M_w/M_n$) of the branches were determined on a Waters SEC system with a 500 mm Jordi DVB linear mixed-bed column and a DRI detector. The instrument was operated using THF as eluent and calibrated with linear polystyrene standards. The absolute weight-average molecular weight of the graft polymers was determined using light-scattering measurements in toluene on a Brookhaven BI-200SM light scattering goniometer.

Chloromethylation. A catalyst solution was prepared by mixing anhydrous aluminum chloride (Aldrich, 99.99%, 0.40 g) and 1-nitropropane (Aldrich, 98%, 10 mL) until dissolution. Dry carbon tetrachloride (20 mL) was then added. Polystyrene (0.50 g) was dissolved in a mixture of 50 mL of dry carbon tetrachloride and 5 mL of CMME. The catalyst solution was added dropwise over a period of several minutes. The reaction was allowed to proceed for 1 h and terminated with 5 mL of glacial acetic acid. The solvent and CMME were removed under vacuum, and the polymer was redissolved in a minimum amount of chloroform. The catalyst was extracted with a 1:1 mixture of acetic acid and water, and the polymer was precipitated in methanol. The chloromethylation level was determined by $^1\text{H-NMR}$ spectroscopy.

Pyrene-Labeling Reaction. The chloromethylated polystyrene (0.30 g) was dissolved in dry DMF (16 mL) at room temperature, and 1-pyrenemethanol was added (2.5 equiv, based on the chloromethylation level of the polymer). Sodium hydride (10 equiv) was then added, the reaction was left to proceed for 20 min, and the flask was placed in a 60 °C oil bath for 3 days. The reaction was terminated by precipitation in methanol. Two reprecipitations in methanol were carried out to purify the product. The absence of unbound 1-pyrenemethanol was verified by SEC analysis using a UV detector. The pyrene content of each sample was determined by UV/visible spectrometry on a Perkin-Elmer Lambda 5 spectrophotometer. The extinction coefficient of 1-pyrenemethanol ($3.93 \times 10^4 \text{ L}\cdot\text{mol}^{-1}\cdot\text{cm}^{-1}$) was used to determine the pyrene concentration in the polymers.

Metal–Halogen Exchange Reaction. To ensure a uniform distribution of pyrene labels throughout the macromolecules, a metal–halogen exchange reaction was performed prior to chloromethylation of some samples. The polymer (0.50 g) was loaded in an ampule, and residual moisture was removed by azeotropic distillations with dry THF. The polymer was then redissolved in 30 mL of dry THF. The exchange process involved addition of an *n*-butyllithium solution (Aldrich, 2.5 M in hexanes, 5 mL) to dry THF (30 mL) at –78 °C in a three-necked flask, and dropwise addition of the polymer solution from the ampule. Five minutes after the addition was completed, the reaction was terminated with water. The solution was evaporated to dryness, the residue was redissolved in toluene, and lithium salts were extracted with a 10% (v/v) HCl/water mixture. The polymer was precipitated in methanol and dried under vacuum.

Nitration of Polystyrene. A linear polystyrene sample ($M_n = 1.2 \times 10^5 \text{ g}\cdot\text{mol}^{-1}$) was nitrated for use as a fluorescence quencher. The nitration procedure, described in the literature, uses fuming nitric acid in a nitrobenzene/1,2-dichloroethane mixture.¹² Following the reaction, the polymer was reprecipitated

Table 1. Molecular Weight, Branching Functionality and Pyrene Content of Polystyrene Samples Investigated^a

sample	$M_w^{\text{br}}/10^3\text{g}\cdot\text{mol}^{-1}$	PDI ^{br}	$M_w^{\text{AGP}}/\text{g}\cdot\text{mol}^{-1}$	f	mol % Py ^b	mol % Py (MHX) ^c
linear	44.0	1.20			4.7	
G0	4.3	1.03	7.4×10^4	16	2.9	
G1	4.6	1.03	7.0×10^5	136	2.9	1.4
G2	4.2	1.04	1.3×10^7	2800	0.93	0.44
G3	4.4	1.05	8.8×10^7	18000		0.92

^a The indices br and AGP refer to the branches and the graft polymers, respectively. ^b Samples not subjected to the metal–halogen exchange reaction. ^c Metal–halogen exchange reaction used prior to chloromethylation.

tated in methanol three times, to remove small molecule impurities. The nitration level of the polystyrene sample (19 mol %) was determined by $^1\text{H-NMR}$ spectroscopy.

Fluorescence Lifetime Measurements. The fluorescence lifetime of the pyrene-labeled samples was measured in THF using single-photon-counting techniques. The equipment used was a Photochemical Research Associates 2000 instrument consisting of a PRA 510 hydrogen flash lamp and a PRA 1551 photomultiplier tube detector. Excitation and emission monochromators were used (Jobin Yvon Model H-10). The flash repetition rate was approximately 30 kHz, the excitation wavelength was set to 346 nm, and the monomer emission was monitored at 398 nm. The data acquisition system was a Tracor Northern TN-7200 multichannel pulse height analyzer interfaced with a personal computer. The pulses sent from the time-to-amplitude converter were collected and sorted into 512 channels of the multichannel analyzer, corresponding to different time intervals. Each sample was excited until $\sim 2 \times 10^4$ photons were collected in the peak channel.

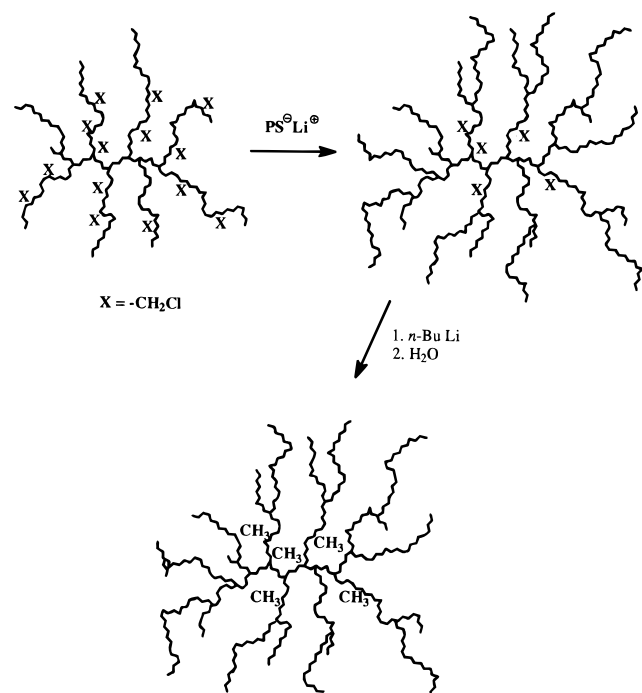
The fluorescence decay data were fitted with a three-exponential function that was convoluted with the lamp pulse. The fitting procedure used a least-squares technique based on the Marquardt–Levenberg algorithm.¹³ The goodness of the fit was judged from the χ^2 parameter, the distribution of the residuals, and the autocorrelation function of the residuals.

Nitrobenzene Quenching Experiments. A quenching solution was prepared at a nitrobenzene concentration of 0.272 M (1.4 mL in 50 mL of distilled THF). Polymer solutions were prepared with a pyrene concentration of approximately $3 \times 10^{-5} \text{ M}$ ($\sim 0.8 \text{ g/L}$ polymer). A 4-mL aliquot of a polymer solution was pipetted into a quartz cuvette and degassed with slow bubbling of nitrogen for 15 min. The fluorescence spectrum was obtained on a Perkin-Elmer MPF-2A spectrofluorometer using an excitation wavelength of 346 nm, the pyrene absorption maximum. The I_5 pyrene monomer emission ($\sim 398 \text{ nm}$) was used to represent the monomer emission intensity. Once the unquenched emission intensity was determined, a 10 μL aliquot of the quencher solution was introduced into the cuvette using a microsyringe. After a 20-min equilibration period, the emission intensity was measured again. The entire process was repeated several times, in order to monitor the emission intensity with respect to quencher concentration.

Nitrated Linear Polystyrene Quenching Experiments. The nitrated linear polystyrene ($M_n = 1.2 \times 10^5 \text{ g}\cdot\text{mol}^{-1}$, 19 mol % NO_2) quenching solution was prepared at a nitro group concentration of 0.011 M (0.13 g in 25 mL of distilled THF). The remainder of the procedure was similar to the nitrobenzene quenching experiments described above, except for using larger quencher aliquots, typically 20–60 μL , necessary to achieve appreciable amounts of quenching.

Results and Discussion

Polymer Samples. The molecular weight and pyrene content of all the polymers used in this work are summarized in Table 1. The abbreviation “MHX” refers to materials subjected to the metal–halogen exchange process. The data presented show that the branches are of uniform size ($PDI < 1.10$ in all cases). The branching functionality of an arborescent polymer of

Scheme 1. Anionic Grafting and Metal–Halogen Exchange Reactions

generation G was calculated from

$$f = \frac{M_w(G) - M_w(G-1)}{M_w(\text{branches})} \quad (1)$$

where $M_w(G)$ and $M_w(G-1)$ refer to the weight-average molecular weight (from light scattering) of arborescent polymers of generation G and of the preceding generation, respectively. The molecular weight and branching functionality of the graft polymers increase in an approximately geometric fashion for successive generations.

The first step in the attachment of pyrene labels to the polystyrene samples is the introduction of linking sites. Chloromethylation was followed by nucleophilic displacement of the chloride anions from the chloromethylated units by the sodium salt of 1-pyrenemethanol.

The anionic grafting reaction used in the preparation of arborescent polymers relies on nucleophilic displacement of chloride anions by polystyryl anions (Scheme 1). In the synthesis of higher generation arborescent polymers, the accessibility of grafting sites decreases because of overcrowding of the molecules. Incomplete reaction of polystyryl anions with the inner chloromethyl sites results in lower than expected grafting efficiencies and molecular weights for higher generation arborescent polymers. Because of this, a significant quantity of residual chloromethyl groups is also expected near the center of the molecule, as shown in Scheme 1. The presence of residual chloromethyl groups was confirmed by a weak peak at δ 4.5 ppm in the NMR spectrum of higher generation graft polymers. Further chloromethylation of these graft polymers would lead to a nonuniform distribution of chloromethyl groups and, subsequently, of pyrene labels throughout the macromolecules. To avoid this problem, samples of generations 1–3 (most likely to display this effect) were subjected to the metal–halogen exchange process, to remove residual chloromethyl groups from the center of the molecules. Subsequent chloromethylation of the

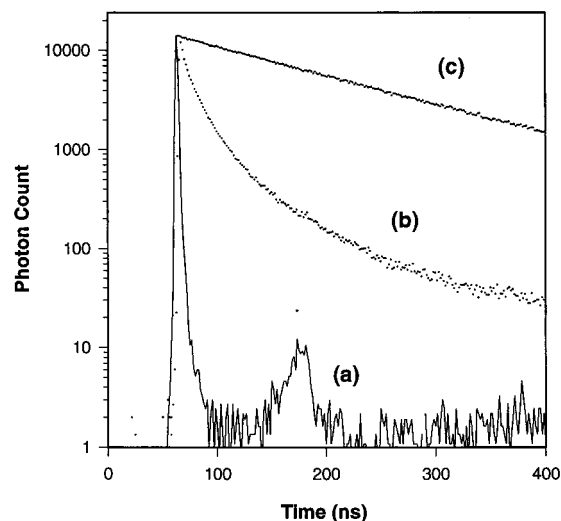


Figure 2. Fluorescence decay profiles: (a) instrumental response; (b) pyrene-labeled arborescent polystyrene; (c) 1-pyrenemethanol.

Table 2. Mean Fluorescence Lifetimes of 1-Pyrenemethanol and Pyrene-Labeled Polystyrenes

sample	$\langle\tau\rangle/\text{ns}$
1-pyrenemethanol	225
linear, 5.4% Py	41.1
G0, 2.9% Py	69.0
G1, 2.9% Py	75.7
G2, 0.9% Py	81.5
G1 (MHX), 1.3% Py	85.1
G2 (MHX), 0.4% Py	112.0
G3 (MHX), 0.9% Py	84.8

exchanged polymers should lead to a uniform distribution of labels throughout the molecules.

Fluorescence Lifetime Measurements. Measurement of the fluorescence lifetime of the pyrene-labeled polystyrenes was the first step in the analysis of their quenching behavior. Comparison of the lifetimes of the polymeric materials with those for the small molecule analog, 1-pyrenemethanol, was carried out in order to determine the effect attachment to polystyrene chains had on the chromophores.

The fluorescence decay profile of 1-pyrenemethanol and of a pyrene-labeled arborescent polymer are compared in Figure 2. Curve a is the instrumental response, curve b is the observed decay profile for a labeled polymer and curve c is for 1-pyrenemethanol. A monoexponential decay is observed for 1-pyrenemethanol. All polymer samples exhibited nonmonoexponential decay behavior. Data fitting using two or more exponential terms was attempted, and it was invariably found that using at least three terms led to much lower χ^2 values than a biexponential model. Considering the complexity of the system, mean fluorescence lifetimes were calculated for the samples using eq 2, where $F(t)$ is the fluorescence intensity at time t .¹⁴ The results of these calculations are presented in Table 2.

$$\langle\tau\rangle = \frac{\int_0^\infty tF(t) dt}{\int_0^\infty F(t) dt} \quad (2)$$

Two distinct effects are apparent in the pyrene-labeled polymers. The average lifetime of polymer-bound chromophores is decreased as compared to unbound 1-pyrenemethanol, because of excimer formation

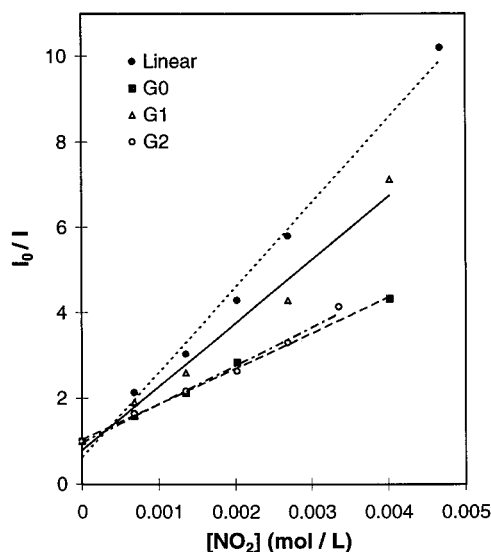


Figure 3. Nitrobenzene quenching of pyrene-labeled polystyrenes.

and backbone quenching. Among the polymer samples investigated, the average lifetimes roughly correlate with the pyrene labeling level and the excimer peak intensity: Samples with higher labeling levels have lower average lifetimes. The decay profile of all pyrene-labeled polymers is also nonmonoexponential. This happens because, in randomly labeled polymers, variations in the distance separating pyrene labels lead to a distribution of excimer formation rate constants and a distribution of lifetimes in the decay profile.

Fluorescence Quenching Experiments. Fluorescence quenching is a process that results in the reduction of fluorescence emission intensity of a chromophore by transfer of excited state energy to another molecule, the quencher species. Pyrene, a common chromophore, was used in combination with two different quenchers. Nitro compounds are known to be efficient quenchers of pyrene fluorescence,¹⁵ and hence nitrobenzene and nitrated linear polystyrene were selected for this work. Nitrobenzene was used to probe the effect of polymer structure on the diffusion rate of small molecules. The nitrated linear polystyrene was used to probe molecular interpenetrability.

The kinetics of steady-state fluorescence quenching are described by the Stern–Volmer equation

$$\frac{I_0}{I} = 1 + k_q \tau_0 [Q] \quad (3)$$

where I_0 and τ_0 are the unquenched fluorescence intensity and lifetime, respectively, I is the fluorescence intensity at quencher concentration $[Q]$, and k_q is the quenching rate constant. For these experiments, the intensity of the pyrene monomer fluorescence was monitored with respect to the quencher concentration. The I_5 monomer emission peak (398 nm) was selected to represent the monomer intensity and the mean unquenched lifetime, $\langle \tau \rangle_0$, was substituted for τ_0 , the unquenched fluorescence lifetime.

Nitrobenzene Quenching. Stern–Volmer plots for nitrobenzene quenching of the pyrene-labeled polystyrenes prepared without the metal–halogen exchange reaction are shown in Figure 3. The good linearity of the plots indicates that the samples obey the Stern–Volmer model. Using the measured lifetimes, the quenching rate constants given in Table 3 were calculated.

Table 3. Nitrobenzene Quenching Rate and Diffusion Constants Calculated from Quenching Experiments with 1-Pyrenemethanol and Pyrene-Labeled Polystyrenes

sample	$k_q/10^{10} \text{ L} \cdot \text{mol}^{-1} \cdot \text{s}^{-1}$	$D/10^{-5} \text{ cm}^2 \cdot \text{s}^{-1}$
1-pyrenemethanol	4.3 ± 0.2	5.2
linear, 5.4% Py	4.3 ± 0.4	5.2
G0, 2.9% Py	1.2 ± 0.1	1.5
G1, 2.9% Py	2.0 ± 0.2	2.4
G2, 0.9% Py	1.0 ± 0.1	1.2
G1 (MHX), 1.3% Py	1.6 ± 0.1	1.9
G2 (MHX), 0.4% Py	1.0 ± 0.1	1.2
G3 (MHX), 0.9% Py	0.9 ± 0.1	1.1

The quenching rate constants for the arborescent samples are up to 4.7 times lower than for the linear sample. This indicates that the arborescent samples have a more dense structure than the linear polymer, and hence more effectively impede diffusion of the quencher. Within the series of samples examined and considering the error limits of the results, the quenching rate constants k_q decrease in the order linear > G1 > G0 > G2 \approx G3. Comparison of the k_q values reported for samples of generations G1 and G2 prepared with and without using the metal–halogen exchange procedure reveals only minor differences. The metal–halogen exchange reaction, used to insure a more uniform distribution of pyrene labels in the molecules, does not seem to lead to very different k_q values. On the basis of these results the metal–halogen exchange reaction, used as an additional precaution, does not seem to be a crucial step in sample preparation. The comb polymer has a k_q value unexpectedly low with respect to the rest of the series. The reason for this deviation is not clear, although it implies a decreased accessibility of the chromophores and therefore an increased segmental density.

The diffusion coefficients calculated for the nitrobenzene quencher in each polymer solution using the Smoluchowski equation (eq 4) are given in Table 3. The effective interaction distance ($\rho = 11 \text{ \AA}$) was calculated from the van der Waals radii of nitrobenzene and pyrene, using Hyperchem 4.51 for Windows, a molecular modeling program.

$$k_q = 4\pi\rho N_A D \quad (4)$$

The results of the nitrobenzene quenching experiments confirm that there are significant differences in segmental density between linear polystyrene and among successive generations of arborescent polystyrenes. Because k_q and D are directly related, the diffusion coefficients for nitrobenzene in solutions of all arborescent samples are also up to 4.7 times smaller than for linear polystyrene and 1-pyrenemethanol. This indicates a marked decrease in the mobility of the quencher in the arborescent polymers and thus an apparent increase in segmental density with increasing generation number. This is consistent with the light-scattering results previously reported, indicating that the arborescent polystyrenes displayed increased structural rigidity over linear polystyrene.⁶ In viscosity measurements, the so-called hydrodynamic density (inversely proportional to the intrinsic viscosity) was similarly observed to increase slightly for successive generations.⁷

Nitrated Linear Polystyrene Quenching. In order to probe the interpenetration of arborescent polystyrenes and linear polymers, a linear polystyrene sample with $M_n = 1.2 \times 10^5 \text{ g} \cdot \text{mol}^{-1}$ and 19 mol % nitration was used to quench the fluorescence of the

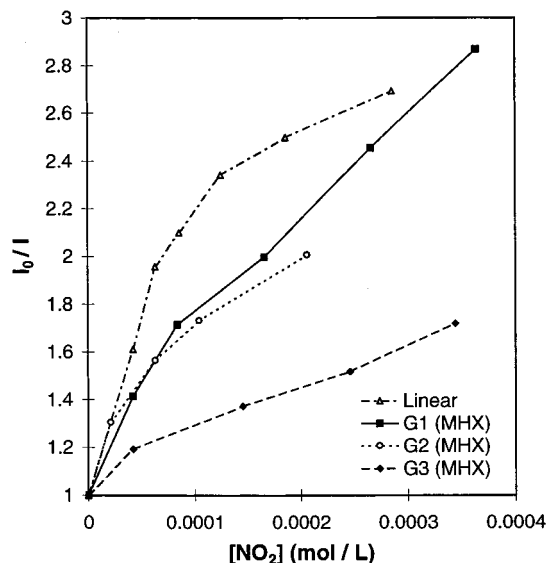


Figure 4. Nitrated polystyrene quenching of pyrene-labeled polystyrenes.

pyrene-labeled samples. The influence of the structure of arborescent polymers on the quenching process was expected to be enhanced in these experiments relative to nitrobenzene quenching, because of the high molecular weight of the quenching species. Stern–Volmer plots for pyrene-labeled samples of linear polystyrene and of the arborescent samples subjected to the metal–halogen exchange reaction are shown in Figure 4. It is clear from the nonlinearity of these curves that the samples do not follow the simpler Stern–Volmer model represented by eq 3. Similar results have been observed in fluorescence quenching of latex particles, where the Stern–Volmer plots displayed downward curvature.¹⁶ This effect was attributed to the unaccessibility of a portion of the chromophores to the quencher molecules. In the present investigation, the pyrene-labeled polymers and nitrated polystyrene quencher are not expected to completely interpenetrate, and should thus lead to a portion of chromophores being inaccessible, explaining the curvature in Figure 4. Correspondingly, a modified version of the Stern–Volmer equation was used, accounting for the fraction of accessible chromophores f_a .¹⁷

$$\frac{I_0}{I_0 - I} = \frac{1}{f_a} + \frac{1}{f_a k_q \tau_0 [Q]} \quad (5)$$

The data from Figure 4 were replotted according to eq 5, to yield the fractional quenching plot shown in Figure 5. In spite of significant data scatter, it seems that the fractional quenching model is appropriate for these systems. The quenching rate constant is obtained from the slope, and the reciprocal of the intercept of each curve represents the fraction of accessible chromophores. The results of the calculations are summarized in Table 4.

The quenching rate constants calculated for the nitrated linear polystyrene quenching are 1 order of magnitude higher than those determined for nitrobenzene quenching, clearly much too large to accurately represent the quenching processes involved. Since the diffusion coefficient of nitrobenzene is presumably much larger than that of the nitrated linear polystyrene, the quenching rate constants of the polymeric quencher should be lower. A possible explanation for the larger than expected k_q values obtained could be the uneven

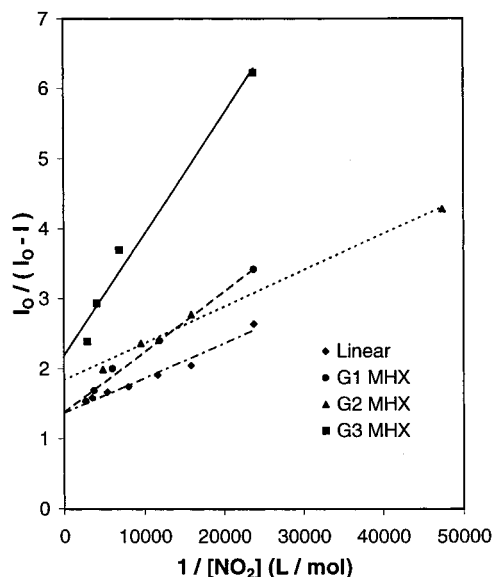


Figure 5. Fractional quenching plot for nitrated polystyrene quenching of pyrene-labeled polystyrenes.

Table 4. Nitrated Linear Polystyrene Quenching Data for Pyrene-Labeled Polystyrenes

sample	$k_q/10^{11} \text{ L} \cdot \text{mol}^{-1} \cdot \text{s}^{-1}$	f_a
linear, 5.4% Py	6.7 ± 0.6	0.73
G1 (MHX), 1.3% Py	1.9 ± 0.2	0.73
G2 (MHX), 0.4% Py	2.9 ± 0.3	0.57
G3 (MHX), 0.9% Py	1.3 ± 0.1	0.46

distribution of NO_2 functionalities in the system. In the nitrobenzene quenching experiments, $[Q]$ represents the bulk concentration of quencher in the solution, since the nitrobenzene molecules are uniformly distributed. In the experiments using nitrated polystyrene, however, the distribution of nitro groups is nonuniform, since their concentration is high inside the linear nitrated polystyrene coil, but zero outside the coil. When a nitrated polystyrene molecule comes in contact with a labeled polymer, the pyrene labels are subjected to a local concentration of nitro groups which is much higher than the bulk concentration. In other words, using the bulk concentration for $[Q]$ in these experiments should lead to an underestimated quencher concentration and therefore an overestimated k_q value. In support of this hypothesis, the local concentration of NO_2 groups inside the nitrated polystyrene coils was estimated. Using $M_n = 1.2 \times 10^5 \text{ g} \cdot \text{mol}^{-1}$ and the Mark–Houwink–Sakurada parameters¹⁸ $k = 0.011 \text{ mL} \cdot \text{g}^{-1}$ and $\alpha = 0.725$ for polystyrene in THF, an intrinsic viscosity $[\eta] = 52.9 \text{ mL} \cdot \text{g}^{-1}$ is obtained. The corresponding hydrodynamic volume of a molecule calculated from the Einstein equation

$$[\eta] = \frac{5}{2} N_A \frac{V_H}{M} \quad (6)$$

using $M = M_n$ is $V_H = 4.2 \times 10^{-21} \text{ L}$. The polymer has a degree of polymerization $X_n = 1.2 \times 10^5 \text{ g} \cdot \text{mol}^{-1}/104.16 \text{ g} \cdot \text{mol}^{-1} = 1150$ and a nitration level of 19 mol %, corresponding to 220 nitro groups or $3.6 \times 10^{-22} \text{ mol}$ per molecule. The local NO_2 concentration inside the coil is, therefore, $0.086 \text{ mol} \cdot \text{L}^{-1}$. All nitrated polystyrene quenching experiments used a bulk $[\text{NO}_2]$ of less than $0.0005 \text{ mol} \cdot \text{L}^{-1}$, about 170 times lower than the concentration inside the coil. On this basis, it seems that using the bulk nitro group concentration for $[Q]$ in eq 5

should lead to an overestimated k_q value, as observed experimentally.

The quenching rate constant for pyrene-labeled linear polystyrene (Table 4) is the highest of all samples, another testament to its lower segmental density. The quenching rate constants for the materials prepared with the metal–halogen exchange do not follow the same pattern observed in the nitrobenzene quenching experiments. The rate constant for the G2 sample is significantly higher than for the G1 and G3 polystyrenes, although significant scatter of the data points may make the results less meaningful. Finally, the fraction of accessible chromophores follows the expected trend, f_a decreasing in the order linear \approx G1 > G2 > G3 in the samples investigated. In the linear polymer, 73% of all chromophores are accessible, but only 46% are accessible in the G3 arborescent polymer, presumably because of an increased segmental density.

The techniques used in this study probed mainly *average* effects, resulting from individual contributions of all volume elements of the arborescent polymer molecules ($\langle\tau\rangle$, k_q , D). In the fractional quenching experiments, it was possible to distinguish two components in the molecules (accessible and inaccessible material fractions) contributing to the quenching behavior. A potentially very powerful technique has been suggested¹⁹ to correlate the morphology of heterogeneous systems such as labeled polymer solutions with their fluorescence decay profile in the presence of quencher. The Stern–Volmer equation can be applied to heterogeneous components in dynamic fluorescence measurements, by considering the individual contributions to quenching of the volume elements composing the polymer molecules. A theoretical decay profile in the presence of the quencher can be generated by assuming a specific distribution of segments for the polymer chains and integrating the Stern–Volmer equation over the whole molecular volume. Agreement between the calculated decay profile and the experimental data implies that the segment distribution function (i.e., the morphological model) used is appropriate. The method was successfully demonstrated for linear polymers, by assuming a simple Gaussian chain segment distribution. While the same technique could potentially be useful in investigating the morphology of arborescent polymers, data analysis would, in practice, become considerably more complex than in the linear polymers examined so far. One of the main problems is that, unlike in high molecular weight linear polymers, non-Gaussian effects are observed in arborescent polymers,⁷ as a result of the high branching densities used (*ca.* 10–15 side chains per backbone chain, or one branching point for every 3–5 monomer units). Systematic validation of the simulation technique discussed using arborescent polymers relies on the availability of a new non-Gaussian model for these molecules, which is unfortunately not the case at the present time. Molecular simulation experiments to obtain a segment density distribution model for arborescent polymers are, therefore, required before such experiments can be attempted to confirm the detailed morphology of the molecules.

Conclusions

The fluorescence quenching experiments indicate that the segmental density of arborescent polystyrenes is significantly higher than for linear polystyrene. The diffusion coefficients of nitrobenzene in solutions of the arborescent polystyrenes are about 2–4 times lower

than for linear polystyrene and unbound 1-pyrenemethanol, indicating restricted mobility of the quencher in the arborescent samples. Fluorescence measurements also provided information regarding differences among successive generations of arborescent polymers. The fluorescence quenching experiments with nitrobenzene indicate a generally decreasing trend in the quenching rate constant with increasing generation number, presumably reflecting a higher segmental density. The results of the quenching experiments using nitrated polystyrene do not follow the simple Stern–Volmer model but obey the modified fractional quenching model. The fraction of accessible chromophores decreases for higher generation samples. The quenching rate constants are much lower than for the linear polymer but do not show variations consistent with the results of the nitrobenzene quenching experiments. The reasons for these deviations will be the topic of further investigation.

Acknowledgment. The financial support of the Natural Sciences and Engineering Council of Canada (NSERC) and of the Ontario Centre for Materials Research (OCMR) for this work are gratefully acknowledged. We would also like to thank Professors Jean Duhamel and Mitchell Winnik for helpful suggestions and discussions.

References and Notes

- (1) Present address: Department of Chemistry, McMaster University, Hamilton, ON L8S 4M1, Canada.
- (2) Present address: Hüls AG, D-45764 Marl, Germany.
- (3) For reviews on dendritic polymers, see, for example: (a) Tomalia, D. A.; Durst, H. D. *Top. Curr. Chem.* **1993**, *165*, 193. (b) Voit, B. I. *Acta Polym.* **1995**, *46*, 87.
- (4) Gauthier, M.; Möller, M. *Macromolecules* **1991**, *24*, 4548.
- (5) Tomalia, D. A.; Hedstrand, D. M.; Ferritto, M. S. *Macromolecules* **1991**, *24*, 1435.
- (6) Gauthier, M.; Möller, M.; Burchard, W. *Macromol. Symp.* **1994**, *77*, 43.
- (7) (a) Gauthier, M.; Li, W.; Tichagwa, L. *Polym. Mater. Sci. Eng.* **1995**, *73*, 232. (b) Gauthier, M.; Li, W.; Tichagwa, L. *Polymer*, in press.
- (8) Sheiko, S.; Gauthier, M.; Möller, M. *Macromolecules* **1997**, *30*, 2343.
- (9) See, for example: (a) Cuniberti, C.; Perico, A. *Eur. Polym. J.* **1977**, *13*, 369. (b) Loutfy, R. O. *Macromolecules* **1981**, *14*, 270. (c) Gelles, R.; Frank, C. W. *Macromolecules* **1982**, *15*, 1486. (d) Zhao, C.-L.; Winnik, M. A.; Riess, G.; Croucher, M. D. *Langmuir* **1990**, *6*, 514. (e) Pekcan, Ö.; Egan, L. S.; Winnik, M. A. *Macromolecules* **1990**, *23*, 2210.
- (10) For fluorescence investigations of the structure of dendritic polymers, see, for example: (a) Caminati, G.; Turro, N. J.; Tomalia, D. A. *J. Am. Chem. Soc.* **1990**, *112*, 8515. (b) Gopidas, K. R.; Leheny, A. R.; Caminati, G.; Turro, N. J.; Tomalia, D. A. *J. Am. Chem. Soc.* **1991**, *113*, 7335.
- (11) Linderman, R. J.; Jaber, M.; Gabriel, B. D. *J. Org. Chem.* **1994**, *59*, 6499.
- (12) Gauthier, M.; Eisenberg, A. *Macromolecules* **1989**, *22*, 3756.
- (13) Press, W. H.; Flannery, B. P.; Teukolsky, S. A.; Vetterling, W. T. *Numerical Recipes: The Art of Scientific Computing*; Cambridge: Cambridge, England, 1992; p 523.
- (14) Egan, L. S.; Winnik, M. A.; Croucher, M. D. *Langmuir* **1988**, *4*, 438.
- (15) Ogasawara, F. K.; Wang, Y.; McGuffin, V. L. *Appl. Spectrosc.* **1995**, *49*, 1.
- (16) Winnik, M. A.; Disanayaka, B.; Pekcan, Ö.; Croucher, M. D. *J. Colloid Interface Sci.* **1990**, *139*, 251.
- (17) Lakowicz, J. R. *Principles of Fluorescence Spectroscopy*; Plenum: New York, 1983, p 279.
- (18) Spatorico, A. L.; Coulter, B. J. *Polym. Sci., Polym. Phys. Ed.* **1973**, *11*, 1139.
- (19) (a) Duportail, G.; Froelich, D.; Weill, G. *Eur. Polym. J.* **1971**, *7*, 977. (b) Moldovan, L.; Weill, G. *Eur. Polym. J.* **1971**, *7*, 1023.